Supplementary Information

Table of Contents

1. Experimental methods 1
   a. *TOC1* and *LUX* expression under diel conditions 1
   b. *LHY* and *CCA1* expression under diel conditions 2
2. Transcriptome data on the early kinetics of gene expression in the *lhy/cca1* mutant 3
   a. Transcriptomic results 3
   b. Transcriptomic methods 4
3. Model description 5
   a. Equations 5
   b. Computational methods 8
   c. Parameter values 8
   d. Values of circadian periods 9
   e. Details of equations 10
      i. Morning loop 10
      ii. Evening loop 10
      iii. Equations for COP1 ubiquitin ligase activity 11
   f. Limitations of the model 12
   g. Parameter stability analysis 14
4. Dynamic model behaviour 16
   a. LHY/CCA1 level regulates the circadian period in lhy/cca1 mutants in a dose-dependent manner 16
   b. Regulation of the phase of evening gene expression depends on the EC 17
   c. Role of GI in the evening loop 19
   d. The total abundance of the clock proteins might differ from their activity profiles 20
   e. The change in TOC1 sign in the clock improves the description of the clock mutants 21
   f. Photoperiod sensing by the clock 24
5. Supplemental References 26
6. Supplementary Table 1 (separate file)
7. SBML model file (separate file)

1. Experimental methods

a. TOC1 and LUX expression under diel conditions

Real-time RT-PCR assays of *TOC1* and *LUX* were carried out on *Arabidopsis thaliana* seedlings of accession Ws, *lhy-21 cca1* (Ws), and *lhy-21 cca1 gi-11* (Ws) seedlings (Locke et al, 2006) grown on half-strength Murashige & Skoog media (MS) with 1.2 % agar, without added sucrose. Following 7 days of entrainment under LD cycles of 12h L:12h D at 22°C, seedlings were transferred to 17°C on the same light regime, and on the fifth day seedlings were harvested every two hours into 1 ml of RNAlater (Ambion; Austin, Texas, USA). Lighting was 60 µmol/m^2/s white fluorescent light provided in a Binder (Tuttlingen,

Germany) temperature-controlled incubator. Biological triplicates were independently sampled. Total RNA was extracted (GE Healthcare Illustra RNAspin 96 RNA Isolation Kit, Buckinghamshire, UK) according to manufacturer's instructions. cDNA was synthesized from 1 μg of total RNA (Invitrogen SuperScript VILO cDNA Synthesis kit, Paisley, Scotland) and diluted 1:10 in H_2O. Quantitative PCR reactions were carried out and analysed as previously described (Dixon et al, 2011) in technical triplicate. The standard error of biological replicates was plotted on all graphs. Expression values were normalized to the control transcript *ACTIN 7* (ACT7), amplified with primers 5' CAGTGTCTGGATCGGAGGAT 3' and 5' TGAACAATCGATGGACCTGA 3'. Primers for *TOC1* were as described in (Dixon et al., 2011) and *LUX* primers were 5' TGCTCATCATCTTCACAAACC 3' and 5' CTTCCTCTCCCATTTCAAACTC 3'.

b. LHY and CCA1 expression under diel conditions

Real-time RT-PCR assays of *LHY* and *CCA1* expression were performed on *Arabidopsis thaliana* transgenic *toc1-2* and *toc1-overexpressing (toc1-ox)* plants. The *toc1-2* mutant was described in (Strayer et al, 2000). The *TOC1*-ox line was a gift of the F. Nagy laboratory. It was constructed by cloning a TOC1 cDNA clone, amplified from a cDNA library of wild-type Columbia plants and sequenced to confirm the identity with the published genome sequence, as an XbaI-XhoI fragment into the pPCVB812 binary vector, which contained a 35S promoter for overexpression (Bauer et al, 2004). All DNA manipulations were performed according to standard protocols (Sambrook & Russell, 2001). Agrobacterium-mediated floral dip transformation was performed according to (Clough & Bent, 1998), into a transgenic parent containing the *CAB2:LUC+* reporter, line 6a/2, in the Ws-2 accession (Hall et al, 2001); NASC stock numbers N9352 and N9998). The method of selection of transformants was also described earlier (Bauer et al, 2004). 15-20 independent transgenic lines were tested. Line 118 (shown in Figure 5) does not segregate for the transgene. The parent line described above was tested as the wild-type control.TOC1 expression levels in the *TOC1-ox* and wt control are shown on Supplementary Figure 1. The measurements of *LHY* and *CCA1* expression were done exactly as described in (Locke et al, 2005). Briefly, seedlings were grown under 12L:12D, 20 μmol m^{-2} s^{-1} red light (Sylvania cool white fluorescent tubes covered with a red filter) at 22^{o}C for 6 days. Expression of *LHY* and *CCA1* was measured on the last day of entrainment in two independent biological replicates and in

technical triplicate. The standard error of biological replicates was plotted on all graphs. Primers for *CCA1* and *LHY* were used as in (Edwards et al, 2006).

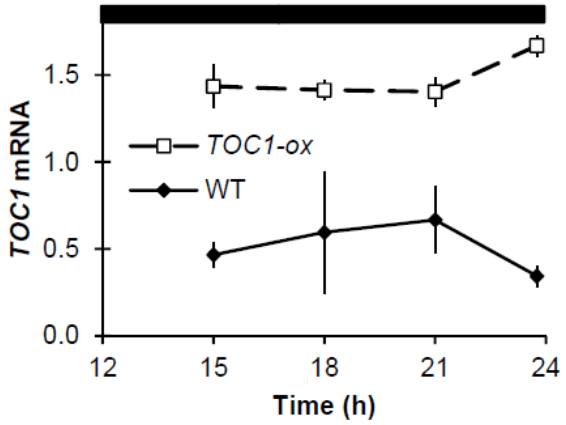

Supplementary Figure 1. The level of TOC1expression in wt and *TOC1*-ox lines. RNA expression analysis by qRT-PCR revealed the expected *TOC1* profile in the WT, dropping towards dawn (24h). The overexpression line (*TOC1*-ox) showed total *TOC1* RNA (native and transgene) at a mean level two to three times the wild-type peak level. Data are means of two biological replicates relative to an *ACT2* control, as in Figure 5. Filled box, darkness

2. Transcriptome data on the early kinetics of gene expression in the *lhy/cca1* mutant

a. Transcriptomic results

Our present and previous models predicted that evening clock genes would show increased expression in the morning in the lhy/cca1 mutant. In particular, genes involved in entraining the evening loop were expected to show increased light responsiveness when the LHY and CCA1 repressors no longer suppressed light induction at dawn. In order to identify such genes, duplicate biological samples were taken from wild type and lhy/cca1 double mutant seedlings from 4 time-points around the night to day transition (-15mins, +15mins, +30mins and +60mins relative to dawn).

The microarray data showed increased expression of the evening genes *LUX*, *ELF4*, *GI* and *TOC1* in the *lhy/cca1* mutant compared to WT, even before dawn (Supplementary Figure 2). Each of the evening genes plotted below also increased its expression after dawn in the mutant but not the WT. This further confirmed our model prediction about the earlier phase of these genes in the *lhy/cca1* mutant. Of all the significantly-regulated genes on the array, *GI* transcript levels were most strongly upregulated by light in the *lhy/cca1* mutant

(Supplementary figure 2C). This early induction of GI contributes to entraining the remnant evening loop in the simulated *lhy/cca1* mutant (as discussed in sections 4b and 4c, below).

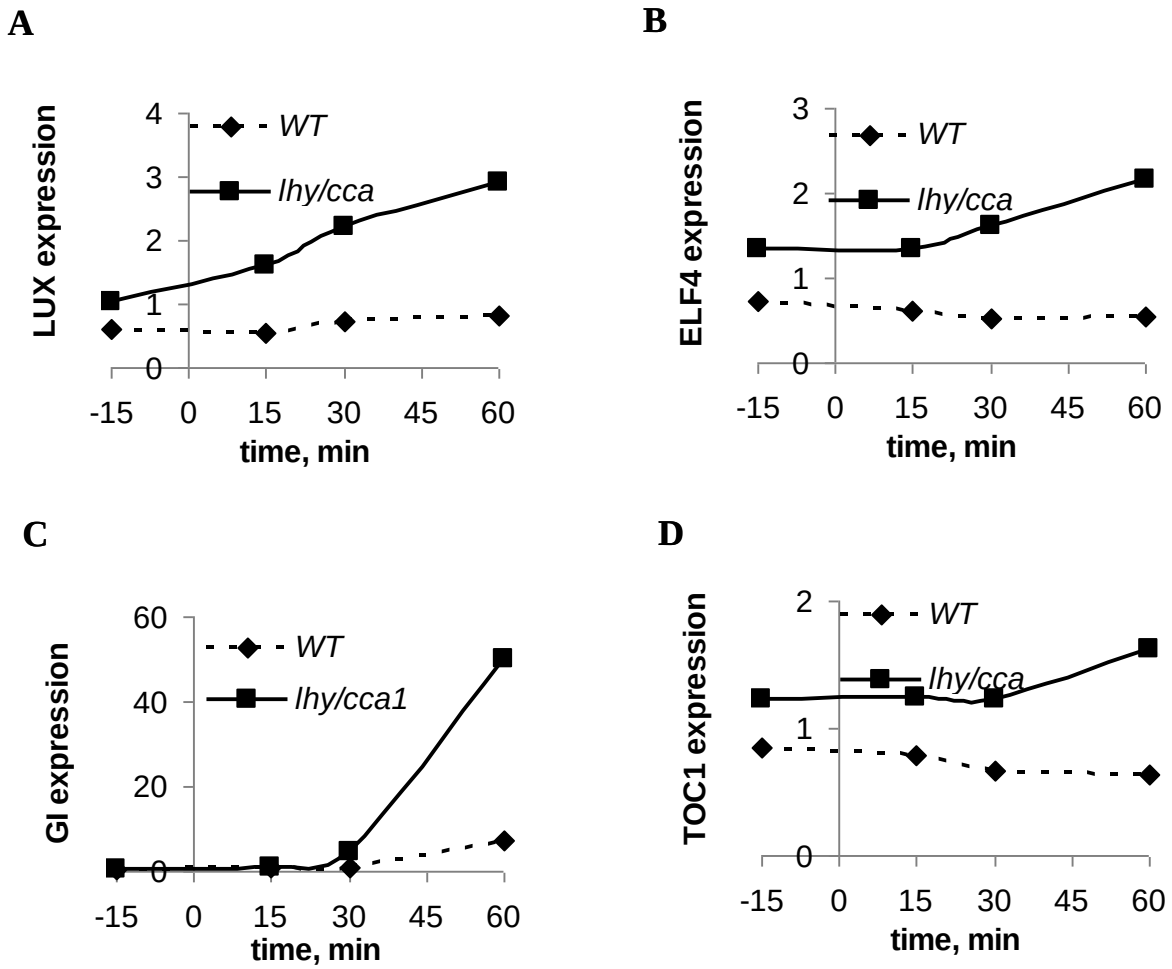

Supplementary Figure 2. The expression of the evening genes increases rapidly at dawn in the *lhy/cca1* mutant. The expression of *LUX*, *ELF4*, *GI* and *TOC1* (A-C) was measured by microarray in the *lhy/cca1* mutant and WT before and after dawn, in plants grown for 9 days under 18L:6D cycles. The data were normalized as described in (Edwards et al, 2006).

b. Transcriptomic methods

Seedlings were grown for 8 days on round Petri dishes (approximately 50 per plate) in Percival I-30BLL growth chambers (CLF Plant Climatics, Emersacker, Germany) under 18h: 6h light dark cycles of 90-95 μmoles $m^{-2}s^{-1}$ cool white fluorescent light at constant 22°C temperature. Plants were harvested before and after dawn on the 9th day of growth. RNA was extracted and analysed by hybridisation to high-density oligonucleotide arrays (Affymetrix ATH1; High Wycombe, UK), as previously described (Edwards et al, 2006). Background correction, normalization and gene expression analysis of the array data were performed

using the GC-RMA routine (Wu et al., 2004) in GeneSpring GX version 7.3.1 (Agilent Technologies, Winnersh, UK). Only genes that could be unambiguously mapped to Arabidopsis transcripts (based on TAIR 7 annotations) were considered in the identification of differentially-expressed genes. Results were filtered to remove non-changing transcripts (< log 2 fold change in expression from the median across all 8 conditions) and those flagged as absent in all 16 individual micro-array chips (according to the MAS5.0 algorithm). Differentially-expressed genes were identified by a 2-way ANOVA, to identify those of the remaining 3517 genes that showed a significant change in expression associated with genotype (WT or *lhy/cca1*) or time, and in particular the five genes with a significant ($P<0.05$) interaction between 'genotype' and 'time'. Benjamini and Hochberg False Discovery Rate correction was applied to reduce multiple testing errors. Four genes showed greater light inducibility in *lhy/cca1:* At1g22770 (*GI*), At1g10760 (*SEX1*), At2g42540 (*Cor15a*) and At1g56300 (DNAJ heat shock protein); At5g06980 showed reduced light inducibility in *lhy/cca1*. Data are available from NASC, dataset number 430, and from ArrayExpress, dataset E-GEOD-19263.

3. Model description

a. Equations

The model, which corresponds to the scheme of the circadian clock from Figure 1 of the Results, is described by the system of ordinary differential equations (ODEs):

$$\frac{dc_L^m}{dt} = q_1 L c_P + n_1 \frac{g_1^{\,a}}{g_1^{\,a} + (c_{P9} + c_{P7} + c_{NI} + c_T)^a} - (m_1 L + m_2 D) \cdot c_L^m \quad (1)$$

$$\frac{dc_L}{dt} = (p_2 + p_1 L) \cdot c_L^m - m_3 c_L - p_3 \frac{c_L^{\,c}}{c_L^{\,c} + g_3^{\,c}} \quad (2)$$

$$\frac{dc_{L\,\mathrm{mod}}}{dt} = p_3 \frac{c_L^{\,c}}{c_L^{\,c} + g_3^{\,c}} - m_4 c_{L\,\mathrm{mod}} \quad (3)$$

$$\frac{dc_P}{dt} = p_7 D \cdot (1 - c_P) - m_{11} c_P L \quad (4)$$

$$\frac{dc_{P9}^m}{dt} = L \cdot q_3 \cdot c_P + \frac{g_8}{g_8 + c_{EC}} \left(n_4 + n_7 \cdot \frac{c_L^{\,e}}{g_9^{\,e} + c_L^{\,e}}\right) - m_{12} c_{P9}^m \quad (5)$$

$$\frac{dc_{P9}}{dt} = p_8 c_{P9}^m - (m_{13} + m_{22}D) \cdot c_{P9} \tag{6}$$

$$\frac{dc_{P7}^m}{dt} = n_8 \frac{{c_{Ltot}}^e}{{g_{10}}^e + {c_{Ltot}}^e} + n_9 \frac{{c_{P9}}^f}{{g_{11}}^f + {c_{P9}}^f} - m_{14} c_{P7}^m \tag{7}$$

$$\frac{dc_{P7}}{dt} = p_9 c_{P7}^m - (m_{15} + m_{23}D) \cdot c_{P7} \tag{8}$$

$$\frac{dc_{NI}^m}{dt} = n_{10} \frac{{c_{L\mathrm{mod}}}^e}{{g_{12}}^e + {c_{L\mathrm{mod}}}^e} + n_{11} \frac{{c_{P7}}^b}{{g_{13}}^b + {c_{P7}}^b} - m_{16} c_{NI}^m \tag{9}$$

$$\frac{dc_{NI}}{dt} = p_{10} c_{NI}^m - (m_{17} + m_{24}D) \cdot c_{NI} \tag{10}$$

$$\frac{dc_T^m}{dt} = n_2 \cdot \frac{g_4}{g_4 + c_{EC}} \cdot \frac{{g_5}^e}{{g_5}^e + {c_L}^e} - m_5 c_T^m \tag{11}$$

$$\frac{dc_T}{dt} = p_4 c_T^m - (m_6 + m_7 D) \cdot c_T (c_{ZTL} \cdot p_5 + c_{ZG}) - m_8 c_T \tag{12}$$

$$\frac{dc_{E4}^m}{dt} = n_{13} \cdot \frac{g_2}{g_2 + c_{EC}} \cdot \frac{{g_6}^e}{{g_6}^e + {c_L}^e} - m_{34} c_{E4}^m \tag{13}$$

$$\frac{dc_{E4}}{dt} = p_{23} c_{E4}^m - m_{35} c_{E4} - p_{25} c_{E4} c_{E3n} + p_{21} c_{E34} \tag{14}$$

$$\frac{dc_{E3}^m}{dt} = n_3 \frac{{g_{16}}^e}{{g_{16}}^e + {c_L}^e} - m_{26} c_{E3}^m \tag{15}$$

$$\frac{dc_{E3c}}{dt} = p_{16} c_{E3}^m - m_9 c_{E3c} c_{COP1c} - p_{17} c_{E3c} c_{Gc} - p_{19} c_{E3c} + p_{20} c_{E3n} \tag{16}$$

$$\frac{dc_{E3n}}{dt} = p_{19} c_{E3c} - p_{20} c_{E3n} - p_{17} c_{E3n} c_{Gn} - m_{30} c_{E3n} \cdot c_{COP1d} - m_{29} c_{E3n} \cdot c_{COP1n} + p_{21} c_{E34} - p_{25} c_{E4} c_{E3n} \tag{17}$$

$$\frac{dc_{LUX}^m}{dt} = n_{13} \cdot \frac{g_2}{g_2 + c_{EC}} \cdot \frac{{g_6}^e}{{g_6}^e + {c_L}^e} - m_{34} c_{LUX}^m \tag{18}$$

$$\frac{dc_{LUX}}{dt} = p_{27} c_{LUX}^m - m_{39} c_{LUX} - p_{26} c_{LUX} c_{E34} \tag{19}$$

$$\frac{dc_{COP1c}}{dt} = n_5 - p_6 c_{COP1c} - m_{27} c_{COP1c} (1 + p_{15} L) \tag{20}$$

$$\frac{dc_{COP1n}}{dt} = p_6 c_{COP1c} - n_6 L \cdot c_P \cdot c_{COP1n} - n_{14} c_{COP1n} - m_{27} c_{COP1n} (1 + p_{15} L) \tag{21}$$

$$\frac{dc_{COP1d}}{dt} = n_{14} c_{COP1n} + n_6 L \cdot c_P \cdot c_{COP1n} - m_{31} (1 + m_{33} D) \cdot c_{COP1d} \tag{22}$$

$$\frac{dc_{EGc}}{dt} = p_{17}c_{E3c}c_{Gc} - m_9c_{EGc}c_{COP1c} - p_{18}c_{EGc} + p_{31}c_{EGn} \quad (23)$$

$$\frac{dc_{EC}}{dt} = p_{26}c_{LUX}c_{E34} - m_{36}c_{EC}\cdot c_{COP1n} - m_{37}c_{EC}\cdot c_{COP1d} - m_{32}c_{EC}(1 + p_{24}\cdot L\cdot \frac{c_{Gn\_tot}^{\ d}}{g_7^{\ d} + c_{Gn\_tot}^{\ d}}) \quad (24)$$

$$\frac{dc_{ZTL}}{dt} = p_{14} - p_{12}Lc_{ZTL}c_G + p_{13}c_{ZG}D - m_{20}c_{ZTL} \quad (25)$$

$$\frac{dc_{ZG}}{dt} = p_{12}Lc_{ZTL}c_G - p_{13}c_{ZG}D - m_{21}c_{ZG} \quad (26)$$

$$\frac{dc_G^m}{dt} = Lq_2c_P + n_{12}\frac{g_{14}}{g_{14} + c_{EC}}\cdot\frac{g_{15}^{\ e}}{g_{15}^{\ e} + c_L^{\ e}} - m_{18}c_G^m \quad (27)$$

$$\frac{dc_{Gc}}{dt} = p_{11}c_G^m - p_{12}Lc_{ZTL}c_{Gc} + p_{13}c_{ZG}D - m_{19}c_{Gc} - p_{17}c_{E3c}c_{Gc} - p_{28}c_{Gc} + p_{29}c_{Gn} \quad (28)$$

$$c_{E34} = p_{25}c_{E4}c_{E3n}/(p_{26}c_{LUX} + p_{21} + m_{37}c_{COP1d} + m_{36}c_{COP1n})$$

$$c_{EGn} = (p_{18}c_{EGc} + p_{17}c_{E3n}c_{Gn})/(m_9c_{COP1n} + m_{10}c_{COP1d} + p_{31})$$

$$c_{Gn} = p_{28}c_{Gc}/(p_{29} + m_{19} + p_{17}c_{E3n})$$

$$c_{Gn\_tot} = c_{Gn} + c_{EGn}$$

Where c_i^m and c_i stand for dimensionless concentrations of mRNA and protein, respectively. The time unit is an hour. Index "*i*" labels the molecular components LHY/CCA1 mRNA or protein (L), LHY/CCA1 modified protein (Lmod), total amount of LHY/CCA1 protein (Ltot), TOC1 mRNA or protein (T), mRNA and proteins for PRR9 (P9), PRR7 (P7), NI (NI), ELF4 (E4), LUX (LUX), ZTL protein (ZTL), mRNA for *ELF3* (E3); *GI* (G), cytoplasmic proteins ELF3 (E3c), GI (Gc), COP1 (COP1c), nuclear proteins ELF3 (E3n), GI (Gn), nuclear protein COP1 in two forms – day (COP1d) and night (COP1n), cytoplasmic protein complexes ELF3-GI (EGc), GI-ZTL (ZG), nuclear protein complexes ELF3-GI (EGn), ELF3-ELF4 (E34), ELF4-ELF3-LUX (EC) and total amount of GI protein in nucleus (Gn_tot). The parameters n_j, m_j represent the rate constants of transcription and degradation, respectively; p_j are constants of translation, protein modification, protein complex formation and translocation between nucleus and cytoplasm; g_j are Michaelis-Menten constants and *a, b, c, d, e ,f* are Hill coefficients; q_j are the rate constants of acute (P-dependent) light activation of transcription. The acute light response in activation of *PRR9, LHY/CCA1, GI*

transcription was modeled analogous to (Locke et al, 2006) using a light-sensitive activator – protein P (c_P), which is accumulated in darkness and was degraded in light. L=1 when light is present, 0 otherwise; D=1-L. The $\theta(t)$ function was used to simulate the smooth transitions between L and D analogous to P2010:

$$L(t) = 0.5 \cdot ((1 + \tanh((t - 24 \cdot floor(t/24) - dawn)/T)) - (1 + \tanh((t - 24 \cdot floor(t/24) - dusk)/T)) + (1 + \tanh((t - 24 \cdot floor(t/24) - 24)/T)))$$

Where *dawn* and *dusk* are the phases of dawn and dusk (normally *dawn=0*); T is the duration of twilight (we used T=0.05 h); tanh and floor – standard functions of hyperbolic tangent and rounding operation.

The introduction of the protein complexes between GI, ELF3, ELF4, LUX increased the number of equations. To simplify the system further, here we used quasi-steady state approximations for the nuclear complexes ELF3-GI, ELF3-ELF4 and nuclear GI protein by assuming the simple fast re-distribution between these species and other protein components.

b. Computational methods

The equations were solved using MATLAB, integrated with the stiff solver ode15s (The MathWorks UK, Cambridge). An SBML version of the model will be available from the Molecular Systems Biology website (www.nature.com/msb) , the Biomodels database (Le Novere et al, 2006) (accession number MODEL1109200000) and the Plant Systems Modelling repository (www.plasmo.ed.ac.uk). MATLAB versions of the model are available from PlaSMo and from the corresponding author upon request.

c. Parameter values

Parameter values were either constrained based on the available data or fitted to multiple timeseries data sets (see Supplementary Table 1). In total, 43 parameters were constrained and 61 parameters were fitted. The constrained parameters were estimated from timeseries data of the clock *mRNAs* or proteins: LHY/CCA1 (g_3, p_1, p_2, p_3, m_1, m_2, m_3, m_4, c), TOC1 (g_4, g_5, m_5, e), PRR9 (n_4, m_{12}, g_8, g_9, q_3), PRR7 (m_{14}), PRR5 (m_{16}), ELF4 (g_6), ELF3 (g_{16}), LUX (m_{34}), GI (g_{15}, q_2), ZTL (p_{13}, m_{20}, m_{21}), COP1d and COP1n (n_5, n_6, n_{14}, m_{27}, m_{31}, m_{33}, p_6, p_{15}) and HY5 and HFR1 proteins (p_{22}, p_{30}, m_{25}, m_{28}; m_{29}; used only for COP1 parameter

optimization, see below). Parameters of protein P (p_7, m_{11}) were taken from P2010. Parameters, that were directly measured or estimated from the experimental data, namely n_4, m_1, m_2, m_3, m_4, m_5, m_{12}, m_{14}, m_{16}, m_{20}, m_{21}, m_{25}, m_{28}, m_{34}, m_{38}, p_1, p_2, p_{22}, p_{30}, g_5, g_6, g_9, g_{15}, g_{16}, a, b, e, f have higher confidence than the rest of the parameters. The fitting procedure minimized the deviation of simulated mRNA profiles from normalized experimental data from WT plants, entrained in 12L:12D cycles, for the following genes: *LHY* and *CCA1* (Edwards et al, 2010; Farre et al, 2005), *PRR9* and *PRR7* (Helfer et al, 2011; Nakamichi et al, 2003), *GI* (Kim et al, 2007; Locke et al, 2005), *TOC1* (Nakamichi et al, 2005), *ELF3* (Dixon et al, 2011), *LUX* (Hazen et al, 2005; Helfer et al, 2011), *ELF4* (McWatters et al, 2007).

The number of reactions described with Hill kinetics was reduced compared to P2010 to simplify the system. All the Hill coefficients (parameters a, b, c, e, f) were set to 2, which corresponded to the data on the observed dimerization of the clock proteins (Fujiwara et al, 2008; O'Neill et al, 2011; Wang et al, 2010; Yakir et al, 2009). The Hill coefficient for the modulation of the EC degradation by GI (parameter d) was set to 2 for simplicity.

Mutations of the clock genes were simulated by decreasing the rate of the genes transcription to zero for all the null mutants used in our study. The only non-null mutant we used was *cop1*, which was simulated by reducing the *COP1* transcription rate *n5*. Values of *n5* in the range of 1-30% of its WT value gave very similar simulated circadian periods in constant light conditions, between 22.4 and 22.8 h. We chose to use 10% of the WT value of *n5* , which matches the level of COP1 protein in the viable *cop1-4* mutant allele (McNellis et al, 1994).

d. Values of circadian periods

We also fitted the values of free running periods of WT plants in constant light (LL) and constant dark (DD) conditions and periods of the *lhy/cca1*, *toc1* and *ztl* mutants in LL conditions. The period values for the optimal parameters were 24.4 h for WT in LL; 26.5 h for WT in DD; and 17.4 h, 22 h, 26.2 h for the *lhy/cca1*, *toc1* and *ztl* mutants in LL, which correspond to experimental data (Farre et al, 2005; Locke et al, 2005; Mas et al, 2003a; Mas et al, 2003b; Millar et al, 1995a; Strayer et al, 2000).

Additionally to the fitted period data of the above mutants, the optimal parameter set provided good qualitative description of the period data for *prr7/prr9*, *cop1* and *gi* mutants

without fitting. The period values of the *prr7/prr9*, *cop1* and *gi* mutant in LL conditions were 30.6 h, 22.7 h and 21.8 h, which agrees with observed prolonged period of the *prr7/prr9* mutant (Farre et al, 2005) and the short periods of *cop1* and most *gi* mutants (Gould et al, 2006; Martin-Tryon et al, 2007; Millar et al, 1995b).

e. Details of equations

Model equations for various components of the clock were constructed as described below.

i. Morning loop

The equations for the morning loop components LHY, PRR9, PRR7 and NI (PRR5) are similar to P2010. The only two differences are related with equations for *LHY* and *PRR9* expression. In the equation for *LHY* (eq. 1), TOC1 was introduced as an inhibitor together with the other PRRs instead of being an activator as in P2010. Also, the acute light response in *LHY* expression was assumed to be free from inhibition similarly to the acute light responses of *PRR9* and *GI*, which agrees with our data on the noticeable acute light response of *CCA1* mRNA to light pulses given at different times of the dark period in our experiments with skeleton photoperiods (Pokhilko et al, 2010). In the equation for *PRR9* (eq. 5) we introduced the inhibition of *PRR9* expression by the EC (Dixon et al, 2011; Helfer et al, 2011).

ii. Evening loop

Expression of *ELF3*, *ELF4* and *LUX* (eqs. 13, 15, 18) was assumed to be inhibited by LHY and CCA1 based on the published data (Dixon et al, 2011; Hazen et al, 2005; Li et al, 2011; Portoles & Mas, 2010). In addition, *ELF4* and *LUX* expression is inhibited by the EC (Dixon et al, 2011; Helfer et al, 2011; Kikis et al, 2005). To describe the differential regulation of ELF3 protein by cytosolic and nuclear fractions of COP1 (the description of COP1 equations is presented below), we introduced the cytosolic and nuclear fractions of ELF3 protein (eqs. 16 and 17). The terms for the binding between ELF3, ELF4, LUX proteins are presented in eqs. 14, 17, 19. In addition, the terms for the binding between ELF3 and GI are presented in eqs. 16, 17, 23, 28. The terms for the degradation of ELF3 protein and its complexes by COP1 are presented in eqs. 16, 17, 23, 24. The equation for the EC (eq. 24) also has a term,

which accounts for the acceleration of EC degradation by the total amount of GI. The equation for *GI* expression (eq. 27) is similar to P2010, but it has inhibition by the EC (Dixon et al, 2011; Fowler et al, 1999) instead of the hypothetical inhibition by TOC1 in P2010. The equations for ZTL and ZTL-GI complex (eqs. 25, 26) are taken from P2010. *TOC1* expression (eq. 11) is described as inhibited by LHY/CCA1 (Pokhilko et al, 2010) and the EC (Dixon et al, 2011; Kolmos et al, 2009). The equation for TOC1 protein (eq. 12) is taken from P2010.

iii. Equations for COP1 ubiquitin ligase activity

The equations for different forms of COP1 E3 ligase activities were developed using the approach presented in (Pokhilko et al, 2011). The night form of the COP1 E3 ligase activity (COP1n) was assumed to be quickly inactivated by light through its interaction with photoreceptors, such as CRY1 (Yu et al, 2008). However, fast degradation of COP1 substrates immediately after dawn indicated an existence of a day form of COP1 activity (COP1d) (Duek et al, 2004; Pokhilko et al, 2011). Recent data suggested that COP1d may be related with a CULLIN 4 (CUL4) complex with COP1, where COP1 acts as a scaffold for a CUL4 ubiquitin E3 ligase (Chen et al, 2010; Chen et al, 2006). Here we assumed that both forms are active in the targeted degradation of the EC component ELF3, though the day form is less active for this substrate, resulting in more rapid degradation of ELF3 in the dark. Similarly to (Pokhilko et al, 2011), we described a switch of ligase activities upon light/dark transitions so that COP1n (eq. 21) is more active in the night and COP1d (eq. 22) in the day time. We also introduced the cytoplasmic fraction of COP1 (eq. 20), which is responsible for degradation of cytoplasmic ELF3 protein and its complex with GI. Additionally to the acceleration of COP1d degradation in darkness (Pokhilko et al, 2011), we introduced acceleration of COP1n degradation in the presence of light to account for the observed reduction of COP1 level in the light (von Arnim & Deng, 1994; von Arnim et al, 1997). The equations for COP1 activities are independent of the clock, so the parameters of these equations were constrained from the data on the kinetics of COP1 substrates HFR1 and HY5 proteins upon dark/light transitions similarly to (Pokhilko et al, 2011). The equations for HY5 and HFR1 proteins, which were used only for the optimization of COP1 parameters, are taken from (Pokhilko et al, 2011):

$$dc_{HY5}/dt = p_{22} - m_{38}c_{HY5}c_{COP1d} - m_{25}c_{HY5}c_{COP1n}$$

$$dc_{HFR1} / dt = p_{30} - m_{28} c_{HFR1} c_{COP1n}$$

The optimal parameters of the COP1 equations are presented in the Supplementary Table 1 together with other parameters of the model.

f. Limitations of the model

Similarly to our previous models, this model depends on particular assumptions that arise from the limitations in current knowledge about the mechanisms of specific connections in the system. Here we discuss the model assumptions from that point of view and outline the level of uncertainty in the model, for morning-expressed components followed by evening-expressed components.

1) *LHY*, *PRR9* and *GI* transcription was assumed to be acutely activated by light after dawn, similarly to our previous models, through a dark-accumulating protein P (suggested to belong to the bHLH transcription factor family (Locke et al, 2005)). The acute light responses are supported by experimental evidence (Ito et al, 2005; Kim et al, 2003; Locke et al, 2005), however the identity and detailed mechanism of protein P action remain to be clarified.

2) The inhibition of the basal transcription of *LHY* and *CCA1* by PRR9, PRR7, PRR5 inhibitors in the model is supported by regulated transgenic mis-expression data (Nakamichi et al, 2010). Light- regulated degradation of *LHY/CCA1* mRNA is supported by multiple data (Yakir et al, 2007) (Edwards et al, 2010) and is described similarly to our previous model (Pokhilko et al, 2010).

3) The experimentally-observed wave of *PRR9, PRR7, PRR5 (NI)* inhibitors of *LHY* and *CCA1* expression is described, as in our previous model, through sequential activation of *PRRs* transcription by each other and by LHY/CCA1 protein (Pokhilko et al, 2010). Although the activation of *PRR9* and *PRR7* transcription by LHY and CCA1 is partially supported by data (Farre et al, 2005), the mechanisms of the sequential regulation of *PRR* gene transcription by LHY and CCA1 and by each other remain to be elucidated. Additionally to the above activation of *PRR* expression, we included the recently-documented inhibition of *PRR9* expression by the EC complex (Dixon et al, 2011; Helfer et al, 2011).

4) *TOC1 (PRR1)* was added to the wave of PRR inhibitors of *LHY/CCA1* based on the timeseries data for *ztl, prr7 prr9* and *toc1* lines, as described in the main text. The mechanistic details of this inhibition are currently under investigation.

5) The experimentally-observed light-regulated translation and modification of LHY/CCA1 protein (Daniel et al, 2004; Kim et al, 2003) was described as in our previous model (Pokhilko et al, 2010).

6) The inhibition of transcription of *TOC1, LUX, ELF4, ELF3* and *GI* by LHY and CCA1 protein is supported by multiple data (Dixon et al, 2011; Harmer & Kay, 2005; Hazen et al, 2005; Kikis et al, 2005; Li et al, 2011; Locke et al, 2005; Portoles & Mas, 2010). Very recent data suggest the involvement of additional proteins, such as DET1 in the regulation of gene expression by LHY and CCA1 (Lau et al, 2011). Further biochemical characterization of the kinetics of DET1 activity, its co-regulators and their modulation by light and the clock will be necessary in order to include them in future clock models. The transcription of *TOC1*, *LUX, ELF4, GI* and *PRR9* is also negatively regulated by EC in our model, which is supported by multiple experimental observations (Dixon et al, 2011; Fowler et al, 1999; Helfer et al, 2011; Kikis et al, 2005; Kolmos et al, 2009).

7) The light-regulated degradation of PRR9, PRR7, PRR5 (NI) and TOC1 proteins is supported by multiple data data (Farre & Kay, 2007; Ito et al, 2007; Kiba et al, 2007; Kim et al, 2007) and described as in our previous model (Pokhilko et al, 2010).

8) The model describes the formation of protein complexes between ELF3 and ELF4, ELF3 and GI, and between ELF3, ELF4, LUX (EC), which is based on experimental observations (Nusinow et al, 2011; Yu et al, 2008). The exact mechanisms of the formation of these complexes and their functional significance need to be further elucidated.

9) The details of the post-translational regulation of ELF3 protein complexes are unknown. In our model we assumed that they are regulated by different forms of the COP1 ubiquitin E3ligase based on the recent data (Chen et al, 2010; Pokhilko et al, 2011; Yu et al, 2008). The dynamics of COP1-containing complexes await further elucidation, because the function of COP1 has recently been re-evaluated (Chen et al, 2010).

10) The experimentally-observed, light-regulated interactions between GI and ZTL proteins (Kim et al, 2007) were described as in our previous model (Pokhilko et al, 2010). The mechanism of regulation of the Evening complex by GI might involve additional clock components (F box proteins) and needs future research.

Key to informing future models will be measurements of the stoichiometry, modification, dynamics and abundance of multi-protein complexes. Such data have only recently become available for the mammalian clock (Lee et al, 2011).

g. Parameter stability analysis

The robustness of the model to parameter variations was measured under 10 % changes of each parameter. Supplementary Figure 3 shows that less than 3 % changes in the period and less than 10 % change in the amplitude of *LHY* mRNA were observed in constant light conditions for simulated wild-type plants, demonstrating some improvement of the model robustness compared to our previous models (Pokhilko et al, 2010).

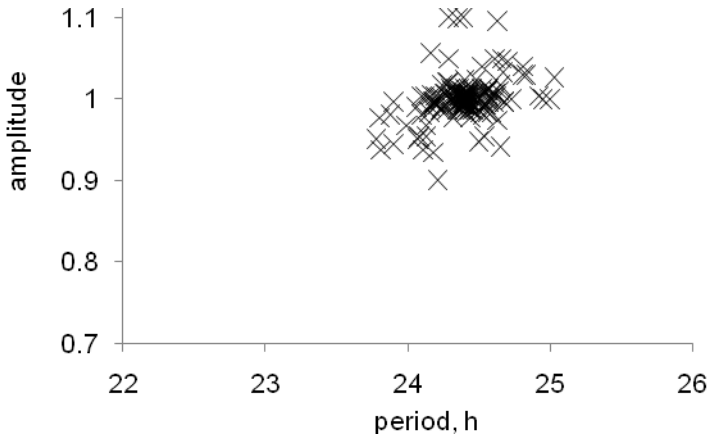

Supplementary Figure 3. The change in the relative amplitude and period of *LHY* mRNA in constant light conditions measured under 10% increase and decrease of each parameter.

Next we demonstrated that variation of parameters does not change the main conclusions of our paper, as the key model behaviours are all retained. The periods of wt and *ztl*, *toc1*, *prr7/prr9* and *lhy/cca1* mutants are preserved under changes of parameters (Supplementary Figure 4 A). The same holds for behaviours present in the previous models, such as the early phase of gene expression in the simulated *lhy/cca1* double mutant, and also for multiple new

features: the suppression of gene expression in the simulated *lhy/cca1/gi* triple mutant because of the loss of indirect activation of gene expression by GI; low amplitude and longer period of the simulated *ztl* mutant and very long period of the *prr7/pp9* double mutant, resulting from the suppression of *LHY/CCA1* expression by TOC1; and arrthythmicity and low amplitude of the *elf3* mutant resulting from the indirect suppression of *LHY/CCA1* expression by loss of the EC. Supplementary Figure 4 illustrates the stability of selected behaviours. Supplementary Figure 4B shows that the simulated *ztl* mutant has 1.1-2.3 h longer period and 1.3-1.7-fold smaller amplitude compared to wt for all the varied parameters. The long period of simulated *prr7/prr9* double mutants under varied parameters is shown in Supplementary Figure 4A. The reduction of peak *LUX* gene expression in *lhy/cca1/gi* compared to *lhy/cca1* is shown in Supplementary Figure 4C.

The above analysis also allowed us to determine the most sensitive parameters of the model, namely n_3, n_5, n_{12}, n_{13}, m_1, m_3, m_5, m_{18}, m_{19}, m_{26}, m_{34}, m_{37}, p_{11}, p_{16}, p_{17}, p_{24}, a, d, g_1, g_2, g_5, g_6, g_{10} and g_{14}. These parameters determine the levels of LHY/CCA1, ELF3, GI mRNA and proteins; *LUX*, *ELF4*, *TOC1* mRNA and the EC. The parameters, which determine the level of each individual PRR mRNA and proteins had less effect on the whole system behaviour, confirming the redundancy of *PRR9*, *PRR7* and *PRR5*, resulting in a spreading of their control of *LHY/CCA1* mRNA over all three genes, consistent with the data (Nakamichi et al, 2010; Nakamichi et al, 2005). In conclusion, the stability analysis demonstrated that the model properties are preserved under variation of parameters.

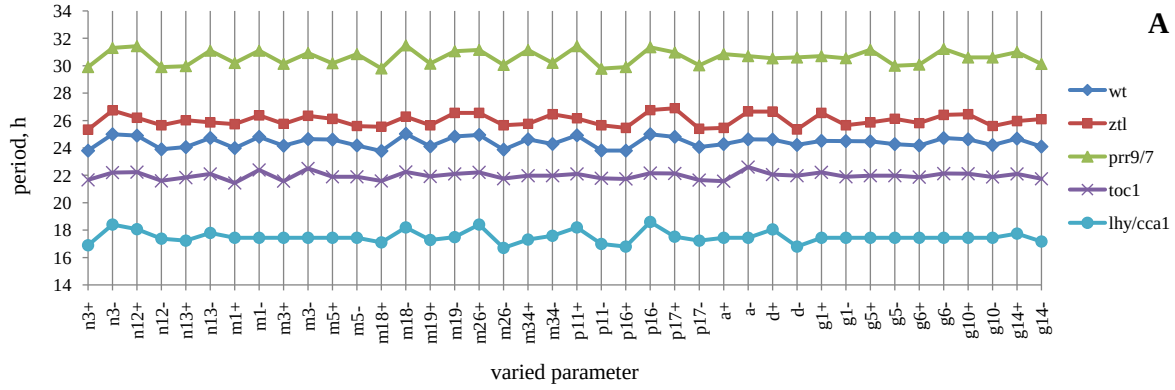

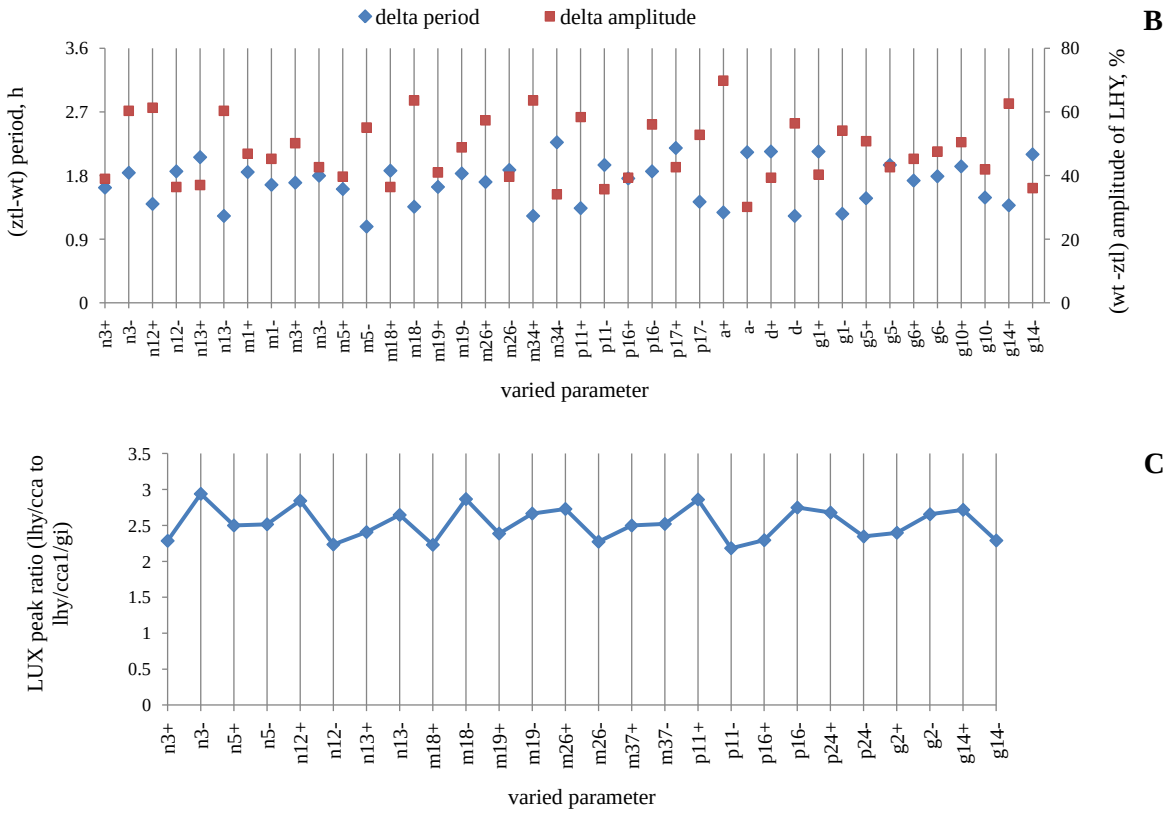

Supplementary Figure 4. Variation of the model characteristics under 10% change in parameters. Only the parameters that caused substantial changes are shown. A: The periods of wt and *ztl*, *toc1*, *prr7/prr9*, *lhy/cca1* mutants under constant light conditions. B: The increase of the period and decrease of the amplitude of the *ztl* mutant relative to wt for constant light conditions. The deviation of the *ztl* amplitude from WT is shown as a % from WT value. C: The ratio of peak *LUX* mRNA levels between *lhy/cca1/gi* and *lhy/cca1* mutants in 12L:12D conditions. The increase or decrease of a parameter value is indicated by "+" and "-" along with the parameter name on the x axis.

4. Dynamic model behaviour

a. LHY/CCA1 level regulates the circadian period in lhy/cca1 mutants in a dose-dependent manner

The model suggests that the absence of the delay in the evening gene expression by LHY and CCA1 dramatically shortens the period of the *lhy/cca1* null mutant, which corresponds to the data (Locke et al, 2006; Locke et al, 2005). To analyse the effect of

LHY/CCA1 level on the clock period in more detail, we simulated partial *lhy/cca1* mutants by a gradual decrease of the *LHY/CCA1* transcription rate. Supplementary Figure 5 shows the dependence of the clock period and *LHY/CCA1* mRNA level on the rate of *LHY/CCA1* transcription. *LHY/CCA1* transcription rates below 30% of WT (corresponding to 50% reduction of *LHY/CCA1* mRNA level) are required to cause significant shortening of the period, consistent with the relatively mild, 1-2h short period phenotype of *lhy* or *cca1* single mutants (Gould et al, 2006; Mizoguchi et al, 2002; Yakir et al, 2009) compared to *lhy/cca1* double mutants.

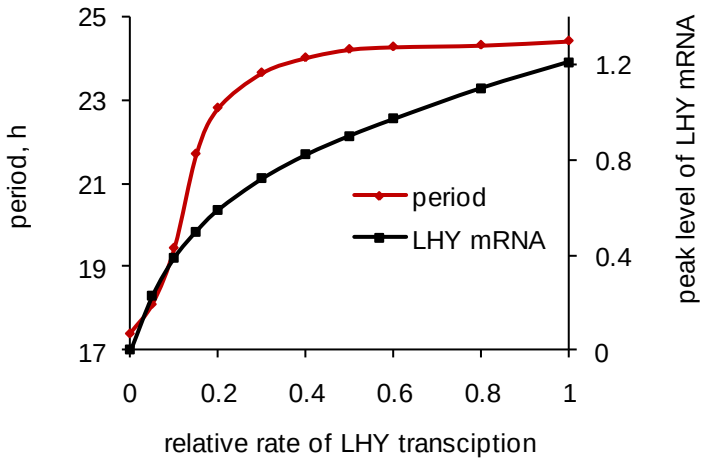

Supplementary Figure 5. Dependence of the clock period on the relative rate of *LHY/CCA1* transcription in the model under constant light conditions. The period of the evening genes (red) is shown together with the peak level of *LHY/CCA1* mRNA (black). Zero rate of *LHY/CCA1* transcription corresponds to the *lhy/cca1* null mutant.

b. Regulation of the phase of evening gene expression depends on the EC

Our data showed the advance in the phase of evening genes *LUX* and *TOC1* in the *lhy/cca1* mutant compared to WT (Figure 2A, B; Supplementary Figure 2), because LHY and CCA1 proteins normally delay the onset of their expression in WT. Model simulations showed that the expression profile of EC-targeted evening genes *ELF4*, *LUX*, *TOC1* and *GI* is also affected by the rise in EC levels at night, which ends their expression peak (Figure 2). In the *lhy/cca1* mutant, this regulation drives rhythmicity in the remnant clock circuit (Supplementary Figure 6 shows *LUX* as an example of the evening gene). The simulated EC kinetics, in turn, depends on the targeted degradation of ELF3 protein and its complexes with

LUX and ELF4 proteins by COP1. This degradation delays the accumulation of EC relative to the peaks of *ELF3*, *ELF4* and *LUX* expression. The simulations showed that this delay allows the evening genes to reach peak expression in the morning in *lhy/cca1* double mutant, in agreement with the available data (Hazen et al, 2005; Locke et al, 2005; Mizoguchi et al, 2002). Their expression is then suppressed by the EC, which reaches a peak in the early night (Supplementary Figure 6).

The model assumed that COP1d is the main regulator of ELF3 and hence the EC in the day time, so the falling level of COP1d at the end of the day allows accumulation of the EC (Supplementary Figure 6). EC levels are then reduced during the night by the rising level of COP1n, which is the major regulator of ELF3 at night. We assumed that COP1d has a higher activity towards EC compared to COP1n, causing rapid degradation of ELF3 protein in the day. The reduction of EC levels in the early day causes robust, early expression of the evening genes in the *lhy/cca1* mutant, in line with the data (Figure 2), and thus contributes to entrainment of the evening loop in the mutant. De-repression of *GI* expression in the simulated *lhy/cca1* mutant (Supplementary Figure 2 C) also contributes to suppressing EC levels in the day, as detailed below.

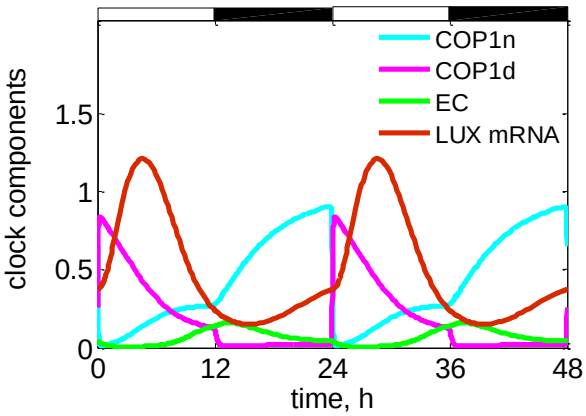

Supplementary Figure 6. The evening gene expression in the simulated *lhy/cca1* double mutant depends on the EC accumulation profile. Model simulations are shown for 12L:12D conditions in the double mutant. The profile of *LUX* mRNA (black) mirrors the EC levels (green), which in turn depend on COP1d (magenta) and COP1n (blue)

c. Role of GI in the evening loop

To study the role of GI in the evening loop, we modelled the clock kinetics in the *lhy/cca1/gi* mutant. In the model, GI reduces EC levels. Removing this negative regulation of the EC by GI would be expected to result in earlier and/or stronger suppression of the evening genes expression by the EC in the *lhy/cca1/gi* triple mutant compared to the *lhy/cca1* double mutant. Indeed, EC levels rise from 2h after dawn in the triple mutant, instead of from 7h after dawn in the double, reducing the peak in expression of the evening genes (represented by *LUX* in Supplementary Figure 7). In constant light conditions this results in the observed arrhythmia of the triple mutant accompanied by lower expression of evening genes than in the double mutant (Supplementary Figure 7), as previously observed for *TOC1* (Locke et al, 2006). In diel cycles the model also predicted a lower expression level of EC target genes in *lhy/cca1/gi* compared to the *lhy/cca1* mutant, as shown on Figure 3 in the main text: thus GI function increases evening gene expression.

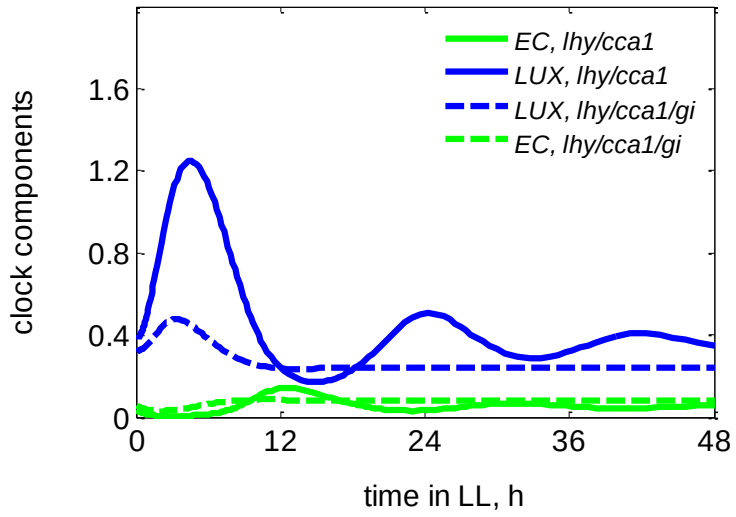

Supplementary Figure 7. GI is necessary for the rhythmicity of the evening loop. Simulations show the increase in the trough level of the EC (green) and reduction in the peak of *LUX* mRNA level (black) in the simulated *lhy/cca1/gi* mutant compared to the *lhy/cca1* mutant. The timeseries are shown for constant light conditions starting at time 0, the time of dawn in the preceding LD cycles.

d. The total abundance of the clock proteins might differ from their activity profiles

Our model included various forms of proteins, such as free ELF3, ELF4, LUX and GI proteins as well as their complexes ELF3-GI, ELF3-ELF4, ELF3-ELF4-LUX (EC). The characteristic profiles of the proteins distribution between complexes depended on the particular conditions. For example, Supplementary Figure 8A shows the simulated profiles of various forms of ELF4. Although free ELF4 protein follows *ELF4* mRNA profile with only a 2 hour delay, the total abundance of ELF4 protein depends of its re-distribution between various forms. Interestingly, the regulatory activity of ELF4 protein (in the EC) is delayed by 4 hours in our simulations compared to the total abundance of ELF4 protein in 12L:12D cycles (Supplementary Figure 8A). The same is true for ELF3 and LUX total proteins, which peak at dusk similarly to ELF4.

The total abundance of ELF3 and GI in the model depends on their interaction, which is followed by degradation of the ELF3-GI complex by COP1. The increase in COP1 activity in constant darkness compared to constant light conditions results in elevated levels of ELF3 (and also GI, not shown) in constant light compared to constant dark (Supplementary Figure 8B), which was observed experimentally (David et al, 2006; Liu et al, 2001). These simulations demonstrate the role of protein-protein interactions in the kinetics of the clock, which was recently emphasized for the mammalian circadian system (Lee et al, 2011).

The detailed kinetic measurements of the activity and abundance of the protein complexes in the plant clock, such as COP1 and GI protein complexes await future elucidation.

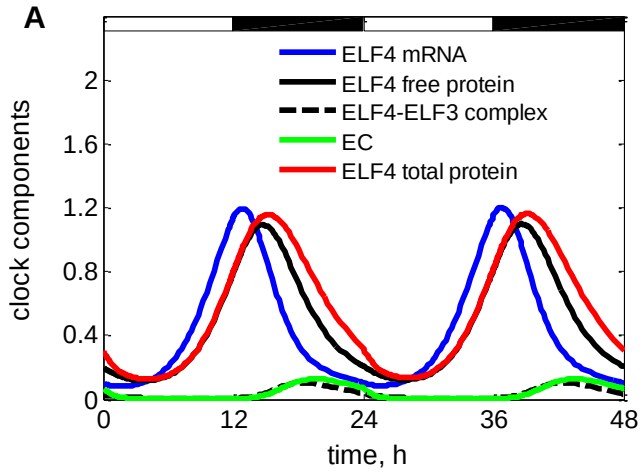

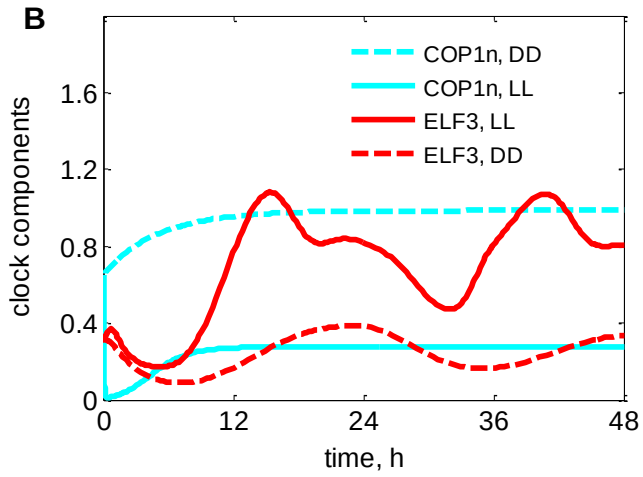

Supplementary Figure 8. Regulation of the total abundance of the clock proteins in the model. A: Re-distribution of ELF4 protein between various forms in 12L:12D cycle; B: Total abundance of ELF3 protein is differently regulated by COP1 activity in constant light and dark conditions. Time 0 corresponds to the transfer of 12L:12D entrained plants into constant conditions.

e. The change in TOC1 sign in the clock improves the description of the clock mutants

In the previous P2010 model TOC1 played the role of on activator of *LHY/CCA1* expression (the direct activator $TOC1_{mod}$ represented the modified TOC1 protein in P2010). This resulted in higher amplitude of *LHY/CCA1* expression in the *ztl* mutant compared to WT in simulations by P2010 model (Supplementary Figure 9A, B), which disagrees with recent data (Baudry et al, 2010). The higher amplitude of *LHY/CCA1* resulted in a higher level of PRR inhibitors in these simulations of the *ztl* mutant (Supplementary Figure 9B), which also contradicts the data on the lower PRR9 and PRR7 levels in the *ztl* mutant compared to WT (Baudry et al, 2010). The new model with TOC1 being an inhibitor of *LHY/CCA1* improved the description of *ztl* as discussed in the main text (Figure 4B).

In addition, description of the *prr9/prr7* double mutant was improved in the new model (Figure 4C) compared to P2010 (Supplementary Figure 9C). The presence of only one inhibitor of *LHY/CCA1* expression (the NI protein) resulted in rapid damping of the oscillations in *prr9/prr7* mutant in P2010 simulations (Supplementary Figure 9C), which disagrees with the data on the robust rhythms of *prr9/prr7* mutants (Farre et al, 2005; Salome & McClung, 2005). The period length of the simulated *prr9/prr7* mutant was only 3 h longer than WT, in contrast to the observed 6-8 h lengthening (Farre et al, 2005; Salome &

McClung, 2005). The robustness of *prr9/prr7* oscillations and the period length were corrected in the present model, as discussed in the main text (Figure 4C). Additionally, the model correctly describes the arrhythmic behaviour of the *prr9/prr7/prr5* triple mutant as a result of the increase in the level of *LHY/CCA1* expression. This provides an additional evidence of the importance of the wave of PRR inhibitors in the clock.

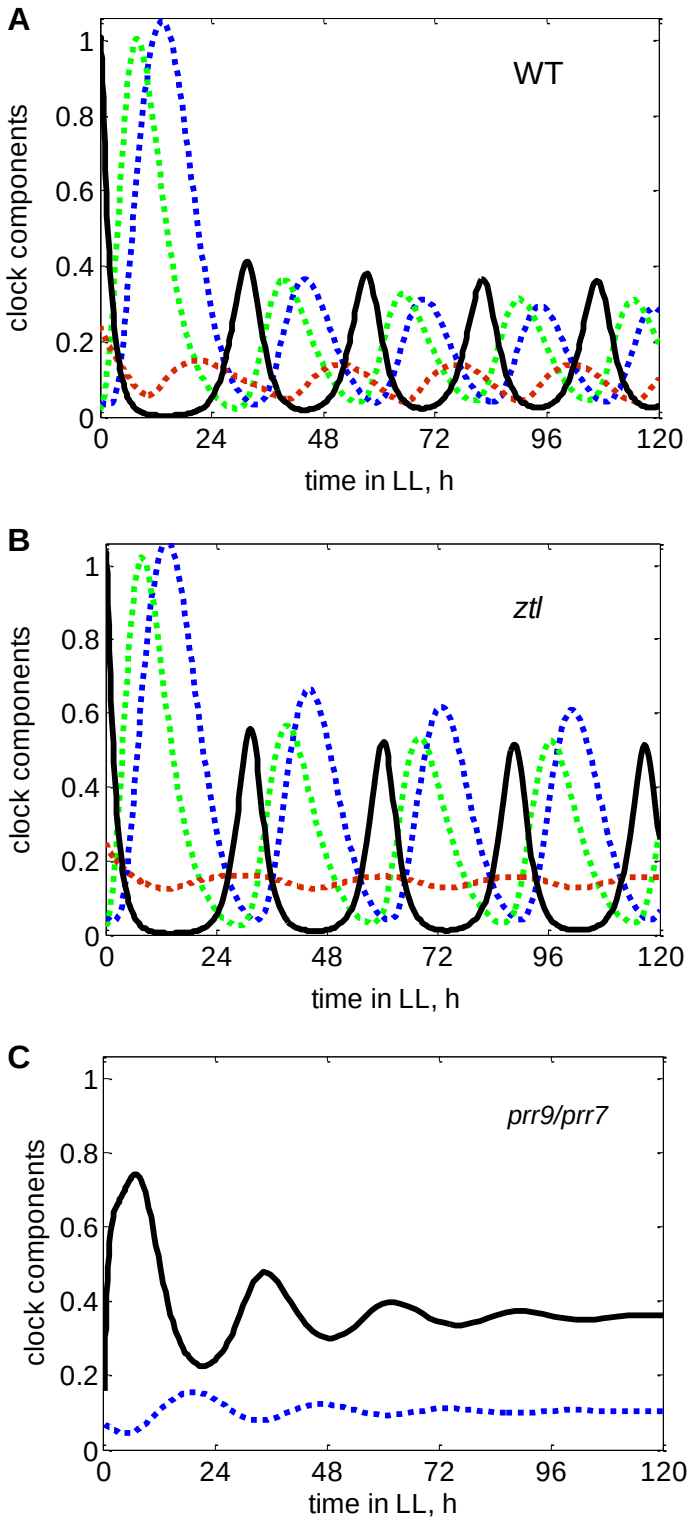

Supplementary Figure 9. Description of *ztl* and *prr9/prr7* mutants with P2010 model in the constant light condition. The level of *LHY/CCA1* mRNA is shown by black lines and PRR7, NI, $TOC1_{mod}$ proteins by green, blue and red correspondingly for WT (A), *ztl* mutant (B) and *prr9/prr7* mutant (C). For the corresponding simulations with the present model, please see Figure 4.

The change of the sign of TOC1 in the clock also allowed us to describe the observed reduction of the amplitude of *LHY/CCA1* oscillations in toc1-overexpressing line (Makino et al, 2002). Thus, the model improves the description of multiple mutants, while retaining its good match to the *toc1* mutant data from P2010. Supplementary Figure 9 shows that the level of *LHY/CCA1* expression is, counter-intuitively, slightly lower in the simulated *toc1* mutant compared to the WT. This is related to the higher trough in the total amount of PRR inhibitors (the sum of PRR9, PRR7, NI proteins). Indeed in WT, *LHY/CCA1* mRNA levels rise only after the decline of TOC1 protein levels (Supplementary Figure 10A). Being the last inhibitor in the wave, TOC1 protein contributes to the low trough of *LHY/CCA1* mRNA in WT. LHY/CCA1 in turn activates the *PRRs* expression, so the low trough of LHY/CCA1 determines the low trough in the *PRRs*. In the *toc1* mutant, however the trough level of *LHY/CCA1* mRNA is de-repressed, and the higher trough level of LHY/CCA1 results in a higher trough in total PRR levels and hence a decrease in the peak level of *LHY/CCA1* expression (Supplementary Figure 10B). The reduction of *LHY/CCA1* mRNA levels in the *toc1* mutant in LD is not pronounced under the current parameter values.

A

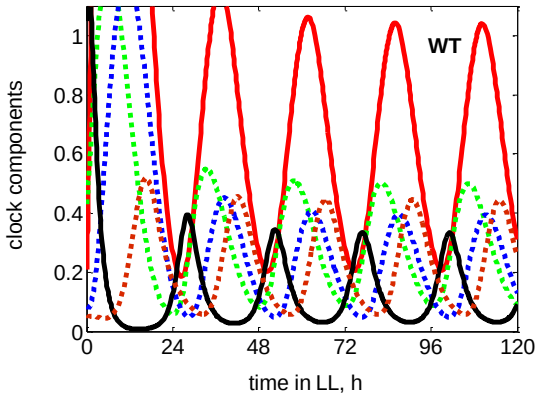

B

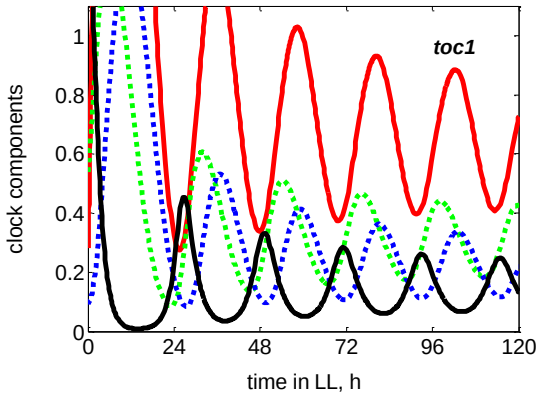

Supplementary Figure 10. The comparison of the current model simulations of WT (A) and the *toc1* mutant (B) in constant light conditions. The level of *LHY/CCA1* mRNA is shown by black lines and PRR7, NI, TOC1 proteins by green, blue and red dotted lines correspondingly. The sum of PRR9, PRR7 and NI proteins is shown as the solid red line,

emphasising the higher trough levels of the *LHY/CCA1* repressors in the *toc1* mutant, and the corresponding decrease in peak *LHY/CCA1* RNA levels.

f. Photoperiod sensing by the clock

Light entrains the plant clock under a wide range of day lengths (photoperiods). Discriminating amongst photoperiods is important for downstream processes, such as flowering (Turck et al, 2008), so changes to clock entrainment under different photoperiods may be physiologically relevant (Salazar et al, 2009). Here we used modelling to explore the main mechanisms of light input to the clock. The P2010 model suggested two mechanisms of photoperiod-dependent entrainment by the clock: 1- through the morning loop, by higher stability of PRR proteins in the light (Farre & Kay, 2007; Ito et al, 2007; Kiba et al, 2007; Mas et al, 2003b); 2 – through the evening loop, by higher *Y* transcription rate in the light, as in the L2005 and L2006 models. The first mechanism was shown to be responsible for the earlier rise of *LHY/CCA1* expression in short days compared to long days (Pokhilko et al, 2010) , which corresponds to experimental observations (Edwards et al, 2010) and is retained in our model (Supplementary Figure 11A). In contrast, the structure of the evening loop and its regulation by light was substantially revised. The EC, which is the main element of the evening loop, is negatively regulated by light through COP1 and GI, as described above. This results in some delay in peak expression of the evening genes under long days in our model simulations. For example, *TOC1* mRNA started to fall only after ZT15 under the 18L:6D photoperiod, which is related with a delay in the rise of its repressor, the EC (Supplementary Figure 11B). However under the 6L:18D photoperiod *TOC1* levels fell after ZT13, because of the earlier rise in the EC (Supplementary Figure 11B). This mechanism improves the model's description of the delayed phase of peak *TOC1* expression under photoperiods greater than 12h (Edwards et al, 2010) compared to the P2010 model, which lacked any analogous mechanism (Supplementary Figure 12).

A

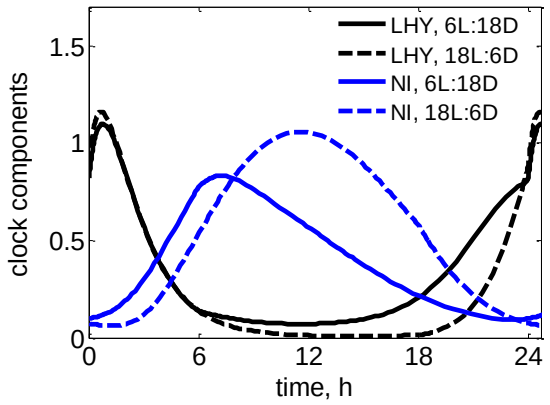

B

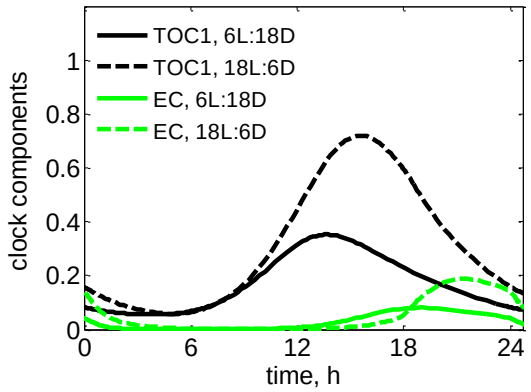

Supplementary Figure 11. Light input to the circadian clock components in WT. Simulated timeseries illustrate the regulation of the morning (A) and evening (B) loops by short and long photoperiods in the model. A: *LHY/CCA1* RNA (black lines) and NI protein (blue lines) expression profiles under short (6L:18D, solid lines) and long (18L:6D, dashed lines) photoperiods . Faster degradation of the *LHY/CCA1* inhibitors in darkness causes an earlier rise of *LHY/CCA1* mRNA level in short days (6L:18D; solid lines) compared to the long days (18L:6D; dashed lines). B: The earlier fall in expression of evening genes (such as *TOC1*, black lines) in the model in 6L:18D (solid lines) is due to an earlier increase in the EC levels (green lines) in darkness, from ZT13.

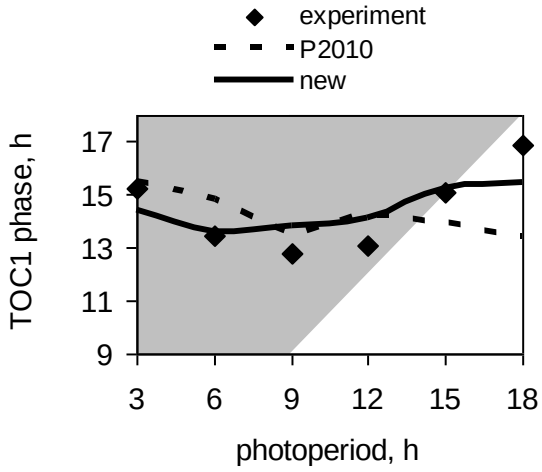

Supplementary Figure 12. Photoperiod sensing by the evening loop. Dependence of peak *TOC1* phase on the day length in WT plants. Simulations are shown by lines for P2010 (dashed line) and current models (solid line). Experimental data points for the peak phase of *TOC1:LUC* reporter expression are taken from (Edwards et al, 2010). Shaded area indicates the time after dusk.

5. Supplemental References

Baudry A, Ito S, Song YH, Strait AA, Kiba T, Lu S, Henriques R, Pruneda-Paz JL, Chua NH, Tobin EM, Kay SA, Imaizumi T (2010) F-box proteins FKF1 and LKP2 act in concert with ZEITLUPE to control Arabidopsis clock progression. *Plant Cell* **22:** 606-622

Bauer D, Viczian A, Kircher S, Nobis T, Nitschke R, Kunkel T, Panigrahi KC, Adam E, Fejes E, Schafer E, Nagy F (2004) Constitutive photomorphogenesis 1 and multiple photoreceptors control degradation of phytochrome interacting factor 3, a transcription factor required for light signaling in Arabidopsis. *Plant Cell* **16:** 1433-1445

Chen H, Huang X, Gusmaroli G, Terzaghi W, Lau OS, Yanagawa Y, Zhang Y, Li J, Lee JH, Zhu D, Deng XW (2010) Arabidopsis CULLIN4-damaged DNA binding protein 1 interacts with CONSTITUTIVELY PHOTOMORPHOGENIC1-SUPPRESSOR OF PHYA complexes to regulate photomorphogenesis and flowering time. *Plant Cell* **22:** 108-123

Chen H, Shen Y, Tang X, Yu L, Wang J, Guo L, Zhang Y, Zhang H, Feng S, Strickland E, Zheng N, Deng XW (2006) Arabidopsis CULLIN4 Forms an E3 Ubiquitin Ligase with RBX1 and the CDD Complex in Mediating Light Control of Development. *Plant Cell* **18:** 1991-2004

Clough SJ, Bent AF (1998) Floral dip: a simplified method for Agrobacterium-mediated transformation of Arabidopsis thaliana. *Plant J* **16:** 735-743

Daniel X, Sugano S, Tobin EM (2004) CK2 phosphorylation of CCA1 is necessary for its circadian oscillator function in Arabidopsis. *Proc Natl Acad Sci U S A* **101:** 3292-3297

David KM, Armbruster U, Tama N, Putterill J (2006) Arabidopsis GIGANTEA protein is post-transcriptionally regulated by light and dark. *FEBS Lett* **580:** 1193-1197

Dixon LE, Knox K, Kozma-Bognar L, Southern MM, Pokhilko A, Millar AJ (2011) Temporal repression of core circadian genes is mediated through EARLY FLOWERING 3 in Arabidopsis. *Curr Biol* **21:** 120-125

Duek PD, Elmer MV, van Oosten VR, Fankhauser C (2004) The degradation of HFR1, a putative bHLH class transcription factor involved in light signaling, is regulated by phosphorylation and requires COP1. *Curr Biol* **14:** 2296-2301

Edwards KD, Akman OE, Knox K, Lumsden PJ, Thomson AW, Brown PE, Pokhilko A, Kozma-Bognar L, Nagy F, Rand DA, Millar AJ (2010) Quantitative analysis of regulatory flexibility under changing environmental conditions. *Mol Syst Biol* **6:** 424

Edwards KD, Anderson PE, Hall A, Salathia NS, Locke JC, Lynn JR, Straume M, Smith JQ, Millar AJ (2006) FLOWERING LOCUS C mediates natural variation in the high-temperature response of the Arabidopsis circadian clock. *Plant Cell* **18:** 639-650

Farre EM, Harmer SL, Harmon FG, Yanovsky MJ, Kay SA (2005) Overlapping and distinct roles of PRR7 and PRR9 in the Arabidopsis circadian clock. *Curr Biol* **15:** 47-54

Farre EM, Kay SA (2007) PRR7 protein levels are regulated by light and the circadian clock in Arabidopsis. *Plant J* **52:** 548-560

Fowler S, Lee K, Onouchi H, Samach A, Richardson K, Morris B, Coupland G, Putterill J (1999) GIGANTEA: a circadian clock-controlled gene that regulates photoperiodic flowering in Arabidopsis and encodes a protein with several possible membrane-spanning domains. *Embo J* **18:** 4679-4688

Fujiwara S, Wang L, Han L, Suh SS, Salome PA, McClung CR, Somers DE (2008) Post-translational regulation of the Arabidopsis circadian clock through selective proteolysis and phosphorylation of pseudo-response regulator proteins. *J Biol Chem* **283:** 23073-23083

Gould PD, Locke JC, Larue C, Southern MM, Davis SJ, Hanano S, Moyle R, Milich R, Putterill J, Millar AJ, Hall A (2006) The molecular basis of temperature compensation in the Arabidopsis circadian clock. *Plant Cell* **18:** 1177-1187

Hall A, Kozma-Bognar L, Toth R, Nagy F, Millar AJ (2001) Conditional circadian regulation of PHYTOCHROME A gene expression. *Plant Physiol* **127:** 1808-1818

Harmer SL, Kay SA (2005) Positive and negative factors confer phase-specific circadian regulation of transcription in Arabidopsis. *Plant Cell* **17:** 1926-1940

Hazen SP, Schultz TF, Pruneda-Paz JL, Borevitz JO, Ecker JR, Kay SA (2005) LUX ARRHYTHMO encodes a Myb domain protein essential for circadian rhythms. *Proc Natl Acad Sci U S A* **102:** 10387-10392

Helfer A, Nusinow DA, Chow BY, Gehrke AR, Bulyk ML, Kay SA (2011) LUX ARRHYTHMO encodes a nighttime repressor of circadian gene expression in the Arabidopsis core clock. *Curr Biol* **21:** 126-133

Ito S, Nakamichi N, Kiba T, Yamashino T, Mizuno T (2007) Rhythmic and light-inducible appearance of clock-associated pseudo-response regulator protein PRR9 through programmed degradation in the dark in Arabidopsis thaliana. *Plant Cell Physiol* **48:** 1644-1651

Ito S, Nakamichi N, Matsushika A, Fujimori T, Yamashino T, Mizuno T (2005) Molecular dissection of the promoter of the light-induced and circadian-controlled APRR9 gene encoding a clock-associated component of Arabidopsis thaliana. *Biosci Biotechnol Biochem* **69:** 382-390

Kiba T, Henriques R, Sakakibara H, Chua NH (2007) Targeted degradation of PSEUDO-RESPONSE REGULATOR5 by an SCFZTL complex regulates clock function and photomorphogenesis in Arabidopsis thaliana. *Plant Cell* **19:** 2516-2530

Kikis EA, Khanna R, Quail PH (2005) ELF4 is a phytochrome-regulated component of a negative-feedback loop involving the central oscillator components CCA1 and LHY. *Plant J* **44:** 300-313

Kim JY, Song HR, Taylor BL, Carre IA (2003) Light-regulated translation mediates gated induction of the Arabidopsis clock protein LHY. *Embo J* **22:** 935-944

Kim WY, Fujiwara S, Suh SS, Kim J, Kim Y, Han L, David K, Putterill J, Nam HG, Somers DE (2007) ZEITLUPE is a circadian photoreceptor stabilized by GIGANTEA in blue light. *Nature* **449:** 356-360

Kolmos E, Nowak M, Werner M, Fischer K, Schwarz G, Mathews S, Schoof H, Nagy F, Bujnicki JM, Davis SJ (2009) Integrating ELF4 into the circadian system through combined structural and functional studies. *Hfsp J* **3:** 350-366

Lau OS, Huang X, Charron JB, Lee JH, Li G, Deng XW (2011) Interaction of Arabidopsis DET1 with CCA1 and LHY in Mediating Transcriptional Repression in the Plant Circadian Clock. *Mol Cell* **43:** 703-712

Le Novere N, Bornstein B, Broicher A, Courtot M, Donizelli M, Dharuri H, Li L, Sauro H, Schilstra M, Shapiro B, Snoep JL, Hucka M (2006) BioModels Database: a free, centralized database of curated, published, quantitative kinetic models of biochemical and cellular systems. *Nucleic Acids Res* **34:** D689-691

Lee Y, Chen R, Lee HM, Lee C (2011) Stoichiometric relationship among clock proteins determines robustness of circadian rhythms. *J Biol Chem* **286:** 7033-7042

Li G, Siddiqui H, Teng Y, Lin R, Wan XY, Li J, Lau OS, Ouyang X, Dai M, Wan J, Devlin PF, Deng XW, Wang H (2011) Coordinated transcriptional regulation underlying the circadian clock in Arabidopsis. *Nat Cell Biol* **13:** 616-622

Liu XL, Covington MF, Fankhauser C, Chory J, Wagner DR (2001) ELF3 encodes a circadian clock-regulated nuclear protein that functions in an Arabidopsis PHYB signal transduction pathway. *Plant Cell* **13:** 1293-1304

Locke JC, Kozma-Bognar L, Gould PD, Feher B, Kevei E, Nagy F, Turner MS, Hall A, Millar AJ (2006) Experimental validation of a predicted feedback loop in the multi-oscillator clock of Arabidopsis thaliana. *Mol Syst Biol* **2:** 59

Locke JC, Southern MM, Kozma-Bognar L, Hibberd V, Brown PE, Turner MS, Millar AJ (2005) Extension of a genetic network model by iterative experimentation and mathematical analysis. *Mol Syst Biol* **1:** 2005 0013

Makino S, Matsushika A, Kojima M, Yamashino T, Mizuno T (2002) The APRR1/TOC1 quintet implicated in circadian rhythms of Arabidopsis thaliana: I. Characterization with APRR1-overexpressing plants. *Plant Cell Physiol* **43:** 58-69

Martin-Tryon EL, Kreps JA, Harmer SL (2007) GIGANTEA acts in blue light signaling and has biochemically separable roles in circadian clock and flowering time regulation. *Plant Physiol* **143:** 473-486

Mas P, Alabadi D, Yanovsky MJ, Oyama T, Kay SA (2003a) Dual role of TOC1 in the control of circadian and photomorphogenic responses in Arabidopsis. *Plant Cell* **15:** 223-236

Mas P, Kim WY, Somers DE, Kay SA (2003b) Targeted degradation of TOC1 by ZTL modulates circadian function in Arabidopsis thaliana. *Nature* **426:** 567-570

McWatters HG, Kolmos E, Hall A, Doyle MR, Amasino RM, Gyula P, Nagy F, Millar AJ, Davis SJ (2007) ELF4 is required for oscillatory properties of the circadian clock. *Plant Physiol* **144:** 391-401

Millar AJ, Carre IA, Strayer CA, Chua NH, Kay SA (1995a) Circadian clock mutants in Arabidopsis identified by luciferase imaging. *Science* **267:** 1161-1163

Millar AJ, Straume M, Chory J, Chua NH, Kay SA (1995b) The regulation of circadian period by phototransduction pathways in Arabidopsis. *Science* **267:** 1163-1166

Mizoguchi T, Wheatley K, Hanzawa Y, Wright L, Mizoguchi M, Song HR, Carre IA, Coupland G (2002) LHY and CCA1 are partially redundant genes required to maintain circadian rhythms in Arabidopsis. *Dev Cell* **2:** 629-641

Nakamichi N, Kiba T, Henriques R, Mizuno T, Chua NH, Sakakibara H (2010) PSEUDO-RESPONSE REGULATORS 9, 7, and 5 are transcriptional repressors in the Arabidopsis circadian clock. *Plant Cell* **22:** 594-605

Nakamichi N, Kita M, Ito S, Yamashino T, Mizuno T (2005) PSEUDO-RESPONSE REGULATORS, PRR9, PRR7 and PRR5, together play essential roles close to the circadian clock of Arabidopsis thaliana. *Plant Cell Physiol* **46:** 686-698

Nakamichi N, Matsushika A, Yamashino T, Mizuno T (2003) Cell autonomous circadian waves of the APRR1/TOC1 quintet in an established cell line of Arabidopsis thaliana. *Plant Cell Physiol* **44:** 360-365

Nusinow DA, Helfer A, Hamilton EE, King JJ, Imaizumi T, Schultz TF, Farre EM, Kay SA (2011) The ELF4-ELF3-LUX complex links the circadian clock to diurnal control of hypocotyl growth. *Nature* **475:** 398-402

O'Neill JS, van Ooijen G, Le Bihan T, Millar AJ (2011) Circadian clock parameter measurement: characterization of clock transcription factors using surface plasmon resonance. *J Biol Rhythms* **26:** 91-98

Pokhilko A, Hodge SK, Stratford K, Knox K, Edwards KD, Thomson AW, Mizuno T, Millar AJ (2010) Data assimilation constrains new connections and components in a complex, eukaryotic circadian clock model. *Mol Syst Biol* **6:** 416

Pokhilko A, Ramos JA, Holtan H, Maszle DR, Khanna R, Millar AJ (2011) Ubiquitin ligase switch in plant photomorphogenesis: A hypothesis. *J Theor Biol* **270:** 31-41

Portoles S, Mas P (2010) The functional interplay between protein kinase CK2 and CCA1 transcriptional activity is essential for clock temperature compensation in Arabidopsis. *PLoS Genet* **6:** e1001201

Salazar JD, Saithong T, Brown PE, Foreman J, Locke JC, Halliday KJ, Carre IA, Rand DA, Millar AJ (2009) Prediction of photoperiodic regulators from quantitative gene circuit models. *Cell* **139:** 1170-1179

Salome PA, McClung CR (2005) PSEUDO-RESPONSE REGULATOR 7 and 9 are partially redundant genes essential for the temperature responsiveness of the Arabidopsis circadian clock. *Plant Cell* **17:** 791-803

Sambrook J, Russell DW (2001) Molecular cloning: A laboratory manual. *Cold Spring Harbor: Cold Spring Harbor Laboratory Press*

Strayer C, Oyama T, Schultz TF, Raman R, Somers DE, Mas P, Panda S, Kreps JA, Kay SA (2000) Cloning of the Arabidopsis clock gene TOC1, an autoregulatory response regulator homolog. *Science* **289:** 768-771

Turck F, Fornara F, Coupland G (2008) Regulation and identity of florigen: FLOWERING LOCUS T moves center stage. *Annu Rev Plant Biol* **59:** 573-594

von Arnim AG, Deng XW (1994) Light inactivation of Arabidopsis photomorphogenic repressor COP1 involves a cell-specific regulation of its nucleocytoplasmic partitioning. *Cell* **79:** 1035-1045

von Arnim AG, Osterlund MT, Kwok SF, Deng XW (1997) Genetic and developmental control of nuclear accumulation of COP1, a repressor of photomorphogenesis in Arabidopsis. *Plant Physiol* **114:** 779-788

Wang L, Fujiwara S, Somers DE (2010) PRR5 regulates phosphorylation, nuclear import and subnuclear localization of TOC1 in the Arabidopsis circadian clock. *Embo J* **29:** 1903-1915

Yakir E, Hilman D, Hassidim M, Green RM (2007) CIRCADIAN CLOCK ASSOCIATED1 transcript stability and the entrainment of the circadian clock in Arabidopsis. *Plant Physiol* **145:** 925-932

Yakir E, Hilman D, Kron I, Hassidim M, Melamed-Book N, Green RM (2009) Posttranslational regulation of CIRCADIAN CLOCK ASSOCIATED1 in the circadian oscillator of Arabidopsis. *Plant Physiol* **150:** 844-857

Yu JW, Rubio V, Lee NY, Bai S, Lee SY, Kim SS, Liu L, Zhang Y, Irigoyen ML, Sullivan JA, Zhang Y, Lee I, Xie Q, Paek NC, Deng XW (2008) COP1 and ELF3 control circadian function and photoperiodic flowering by regulating GI stability. *Mol Cell* **32:** 617-630